

# A Numerical Study on the Performance of a Catamaran-Shaped Floating Breakwater

THEOHARRIS KOFTIS, PANAYOTIS PRINOS  
Hydraulics Laboratory  
Department of Civil Engineering  
Aristotle University of Thessaloniki, 54124, Greece  
GREECE  
[thkoftis@civil.auth.gr](mailto:thkoftis@civil.auth.gr), [prinosp@civil.auth.gr](mailto:prinosp@civil.auth.gr)

*Abstract:* - The efficiency of a catamaran-type fixed floating breakwater (FB) under regular waves is investigated numerically with the use of a 2DV URANS model. This type of structure consists of two immersed vertical barriers that are built as a monolithic structure along with the deck and can be supported on piles. The study is focused on the effect of the immersed vertical barriers of the FB and their spacing on the wave transmission and reflection characteristics. For comparison, a box-type FB is also studied numerically with the same draught as the immersed vertical barriers. It is found that the performance of the catamaran FB is improved considerably with the increase of the relative depth of immersion,  $Dr/D$  ( $Dr$ =Depth of immersed vertical barrier,  $D$ =water depth). Values for the transmission coefficient less than 0.1 are obtained for  $Dr/D > 0.4$ . The efficiency of the box FB is also increased with increasing relative draught, but this influence is less strong than that of the catamaran FB. For  $Dr/D < 0.33$  the catamaran FB is less efficient than the box FB but for higher values of  $Dr/D$  its performance is better. For  $Dr/D > 0.33$ , increased values of the reflection coefficient, greater than 0.7, are obtained for both types of FB. The effect of spacing  $S$  between the two immersed vertical barriers is not significant and resonance can be observed when  $S/L = n/2$ , ( $n=1,2,3,\dots$ ). The detailed velocity field around the structure is presented in order to show the hydrodynamic performance of that type of FB.

*Key-Words:* Wave-structure interaction; Floating breakwater; Wave transmission

## 1 Introduction

Floating Breakwaters (FBs) are environmentally friendly coastal structures that can be used for wave protection of small boat marinas and natural beaches with mild wave conditions. Also for beaches of steep slopes the implementation of floating structures is much more economic than that of founded FBs.

Various studies on the performance of FBs can be found in literature. Bruce and McCartney [1] categorized the various FB types, depending on the materials and type of construction, such as box-type or catamaran shaped FB, their limitations, and some design considerations. Also Isaacson [2] gave some general guidelines for the design process for FBs and the related design criteria with respect to wave effects.

The FB performance is measured with the wave transmission coefficient  $C_t$  ( $=H_t/H_i$ ,  $H_t$ =transmitted wave height,  $H_i$ =incident wave height) which depends on the structure dimensions. For the box shaped FB this coefficient depends strongly on the ratio  $W/L$  ( $W$ = structure length,  $L$ =wave length) and the structure's relative draught  $Dr/D$  ( $Dr$ = draught of FB,  $D$ = water depth) [3].

Both numerical and experimental studies are also available for the catamaran shaped FB. The performance of such a structure was studied numerically by Isaacson et al. [4]. He used an eigenfunction expansion method to perform the numerical calculation and used laboratory results to qualify the energy dissipation within the slotted barrier. He gave results such as transmission and reflection coefficients and the maximum horizontal force on the barrier, for waves from deep to intermediate water. An experimental study for this type of structure was performed by Neelamani et al. [5]. They found that this breakwater is found to be effective when its depth of immersion is of the order of 50% or more of the water depth and especially for high frequency waves.

The purpose of this study is to investigate numerically the effect of the immersed vertical barriers of the FB and their spacing on the wave transmission and reflection characteristics. The relative depth of immersion  $Dr/D$  varies from 0.20 to 0.60 for the catamaran FB. Also, a box FB with the same relative draught is investigated for comparison. Also for the case of  $Dr/D=0.20$  the effect of spacing  $S$  between the two immersed

vertical barriers is examined for values of S/L from 0.25 to 1.50.

Such a study requires a detailed analysis of the flow near the FB, such as 2DV velocity field, turbulence effects, which have not been found in previous numerical studies. The model is based on the 2D-V Unsteady Reynolds Averaged Navier-Stokes (URANS) equations. In this study, the COBRAS (COrnell Breaking Waves and Structures) model, developed by Liu and Lin, is used [6]. The model considers wave reflection, transmission and breaking due to waves and 2DV hydrodynamics properties of the flow near the FB.

## 2 Numerical model

The model solves the 2D-V Unsteady Reynolds Averaged Navier-Stokes (URANS) equations in conjunction with transport equations for  $k$  and  $\epsilon$  for the calculation of the Reynolds stresses. The model uses the Volume of Fluid (VOF) method to “track” the free surface location and the partial cell treatment in order to represent solid objects of arbitrary shape [7]. A brief summary of the boundary, initial conditions and solution procedure used in the COBRAS model is presented in the following paragraphs

### 2.1 Boundary and initial conditions

The dynamic free surface boundary condition is applied for the mean flow velocities, which is equivalent to the zero stress free surface condition if no stresses are applied on the free surface. For the  $k$  and  $\epsilon$  the zero normal gradient boundary condition is applied at the free surface, indicating that turbulence does not diffuse across the free surface. At the rigid boundaries (bed and FB walls) the no-slip condition is applied and the “wall function” approach is implemented at the first near-wall grid point. This avoids a refined modeling of the viscous sub-layer which would be computationally expensive. Also, a low level of turbulent kinetic energy  $k$  is assumed as an initial condition in order to maintain stability as suggested by Lin and Liu [8]. Radiation boundary conditions are set at both sides of the computational domain to allow outgoing waves.

Additionally a sponge layer, an additional exponential damping function term added to the original momentum equation, is imposed at the left boundary, next to the source function, in order to fully absorb the waves that propagate in the opposite direction of the zone of interest.

### 2.2 Wave generation

The waves are generated by the source function method developed by Lin and Liu [9] in a rectangular source at a certain distance from the left side of the domain. The method consists of introducing a pressure variation within the source region cells, in order to generate various types of waves. In this study monochromatic waves have been generated.

### 2.3 Free surface tracking method

The VOF method is used for “tracking” the free surface variation [7]. The donor-acceptor method is used for the free surface reconstruction. The partial cell treatment is used for representing solid objects of arbitrary shape.

### 2.4 Solution procedure

The solution of the URANS equations is based on the two-step projection method, developed by Chorin [10], with the use of the finite difference method. The convection terms in the momentum equations are discretized by a combination of the upwind and central difference scheme in order to produce stable and accurate results. The central difference method is used to express the stress gradient and the pressure gradient and the forward time-differencing method for the time derivatives. Similar expressions are used for the  $k$ - $\epsilon$  transport equations.

## 3 Numerical implementation-Analysis of results

A numerical wave tank, shown in Fig. 1, with dimensions 60m x 2.5 m is used. The grid is uniform with  $\Delta x=8\text{cm}$  and  $\Delta y=4\text{cm}$ . Incident monochromatic waves, with wave height  $H_i = 0.25$  m and wave period  $T=2.04$  sec, are generated with the source function while the water depth in the tank is constant  $D=2\text{m}$ . The source function is located at a distance of 1.5 L from the left side of the domain and 1m above the seabed, with dimensions of  $2\Delta x$  width and  $25\Delta y$  height. The computational time-step, is restricted by the CFL criterion, and takes a maximum value of 0.01 sec. The total computational time for these tests was taken 20T, and the results are presented from 15-20 T when stable condition is obtained.

The dimensions of the catamaran FB examined are shown in Fig. 2. The structure consists of two immersed thin vertical barriers of 20cm width, that

extent below the still water level a distance  $D_r$ , and the distance between them is denoted as  $S$ . The deck along the structure has a width  $W=S+40\text{cm}$ . Also in Fig. 3, a box shaped FB is shown which is used for comparison purposes. The box FB has a width  $W=2.0\text{m}$  and a height  $=0.90\text{m}$ , which correspond to the common used dimensions in prototype scale ( $W=4.0\text{m}$ ,  $=1.80\text{m}$ ) with a scale parameter of 0.5. The dimensions of the wave tank and the FB are those of available large-scale experiments [3].

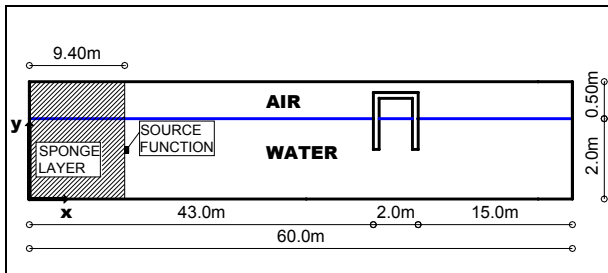


Fig. 1. Numerical wave tank and catamaran FB.

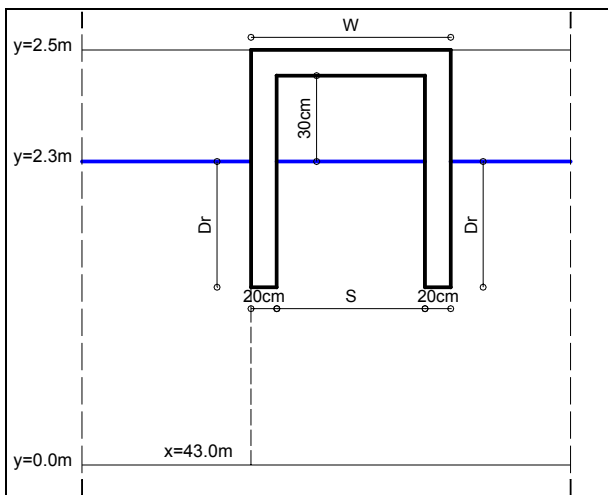


Fig. 2. Definition sketch of catamaran FB.

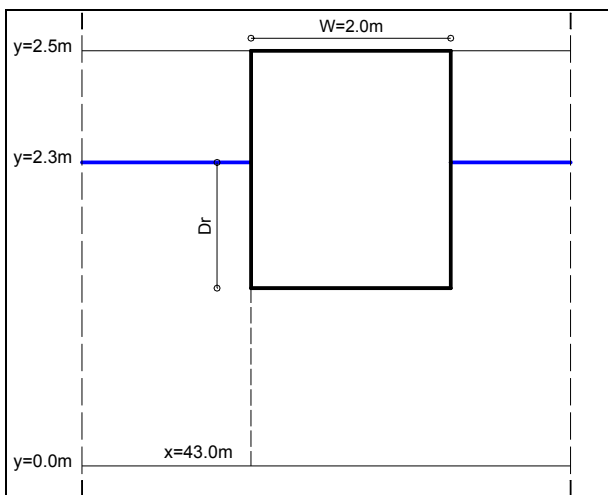


Fig. 3. Definition sketch of box FB.

The numerical model is validated against available experimental data for the box shaped FB [3] and then it is applied to the catamaran shaped FB. Finally, the hydrodynamic properties of the flow in the vicinity of the FB are described in detail.

### 3.1 Wave transmission and reflection characteristics

The reflection and transmission coefficients,  $C_r$  and  $C_t$ , were obtained when the quasi-steady state was reached, calculating the wave heights envelopes as shown in Fig. 4 for example, with  $n_{\max}$  showing the maximum elevation of the free surface and  $n_{\min}$  the minimum. Defining  $H_{\max}=\max\{n_{\max}-n_{\min}\}$  and  $H_{\min}=\min\{n_{\max}-n_{\min}\}$  for a distance about 1-2 wave lengths before the structure, the reflection coefficient is then obtained using

$$C_r = \frac{H_R}{H_{in}} = \frac{H_{\max} - H_{\min}}{H_{\max} + H_{\min}} \quad (1)$$

The transmission coefficient  $C_t$  is calculated using the data of the two gauges shown in Fig. 4 located about 1.5L leeward the structure.

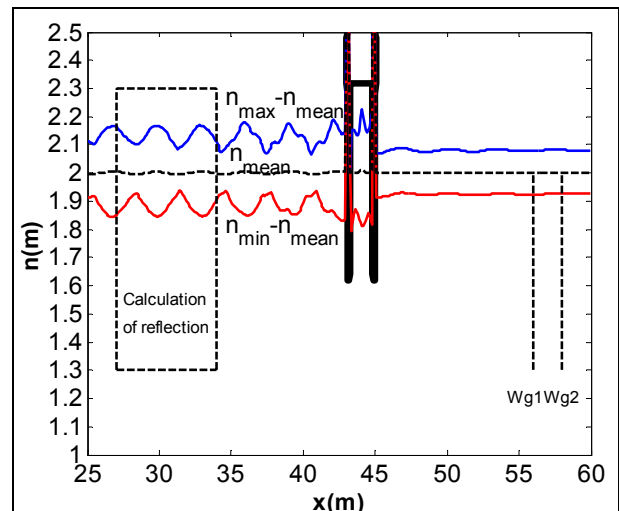


Fig. 4. Wave height envelopes for catamaran FB with  $D_r/D=0.20$ .

#### 3.1.1 Effect of relative depth of immersion

Fig. 5 shows the effect of the relative depth of immersion,  $D_r/D$ , of the catamaran FB with  $S/L=0.25$  and the box FB both with  $W/L=0.32$  on the transmission coefficient together with that of the available experimental data [3]. It can be seen that the influence of  $D_r/D$  is significant for both structures.  $C_t$  decreases with increasing  $D_r/D$ . It should be pointed out that for  $D_r/D < 0.33$  the catamaran's FB performance is worse than that of box FB, while for higher values it is better. It is

noticed that with an increase of  $Dr/D$  from 0.2 to 0.6,  $C_t$  is reduced from 0.33 to 0.07 for the box FB, while it decreases from 0.62 to 0.02 for the catamaran FB.

The variation of the reflection coefficient with the relative depth of immersion has different behavior for the two structures as shown in Fig. 6. For the box FB  $C_r$  does not vary much with  $Dr/D$  and for all configurations  $C_r$  is about 0.72-0.78 showing that box type FB are highly reflective structures. For the catamaran FB the influence of  $Dr/D$  on  $C_r$  is much stronger and an increase of  $Dr/D$  from 0.20 to 0.40 results in an increase of  $C_r$  from 0.35 to 0.76. However for higher values of  $Dr/D$  the variation is not noticeable.

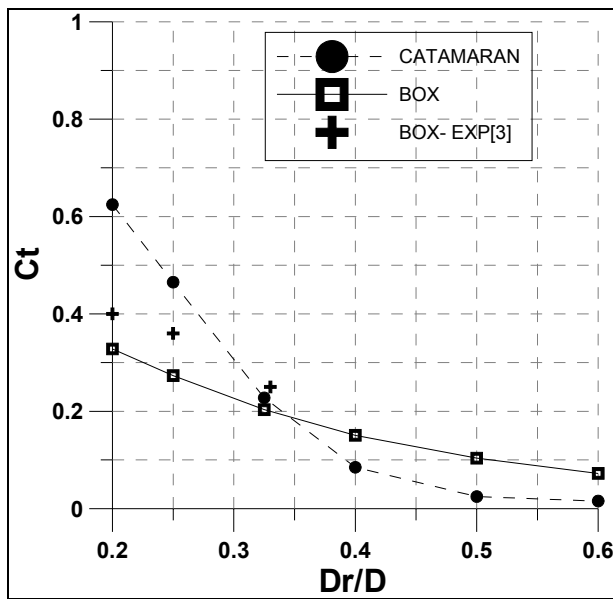


Fig. 5. Variation of  $C_t$  with the  $Dr/D$ .

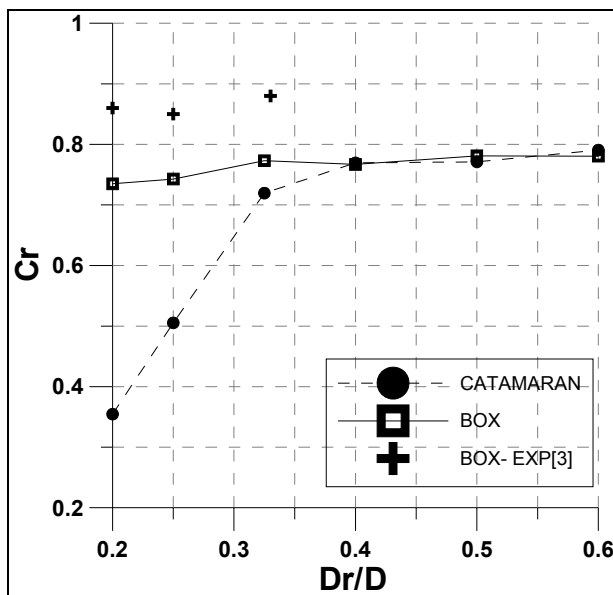


Fig. 6. Variation of  $C_r$  with  $Dr/D$ .

### 3.1.2 Effect of relative spacing

Fig. 7 shows the influence of the relative spacing,  $S/L$ , between the two immersed vertical barriers of the catamaran FB with  $Dr/D=0.20$  on  $C_t$  and  $C_r$ . This effect is stronger on  $C_r$  and resonant excitation can be observed when the  $S/L=n/2$ , ( $n=1,2,3\dots$ ), as stated by Isaacson et al. [4]. For the transmission coefficient the effect is not significant showing that this parameter is not critical in designing a catamaran FB.

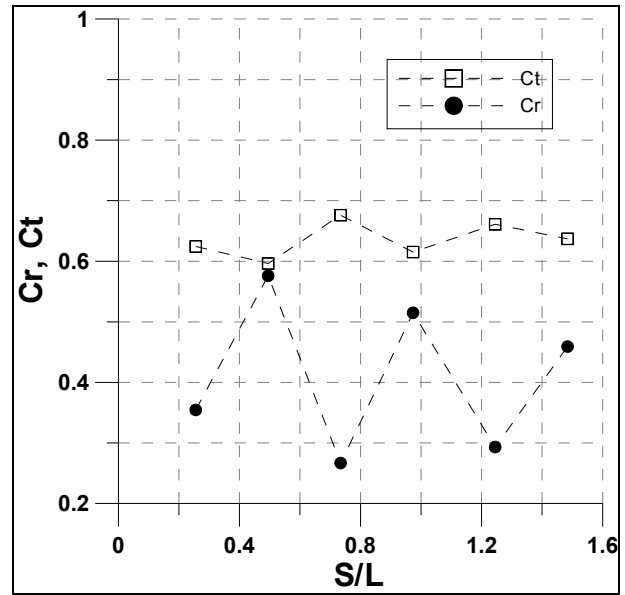


Fig. 7. Variation of  $C_t, C_r$  with  $S/L$ .

### 3.2 Detailed hydrodynamic field

The flow pattern in the vicinity of the catamaran FB, for  $Dr/D=0.2$ , is presented in Fig. 9(a-d) for phases of  $0.25T$  inside a wave cycle from 18-19T. The elevation at both sides of the FB is shown in Fig. 8, with phase a ( $t/T=18.0$ ) corresponding to a wave's trough in the seaward side.

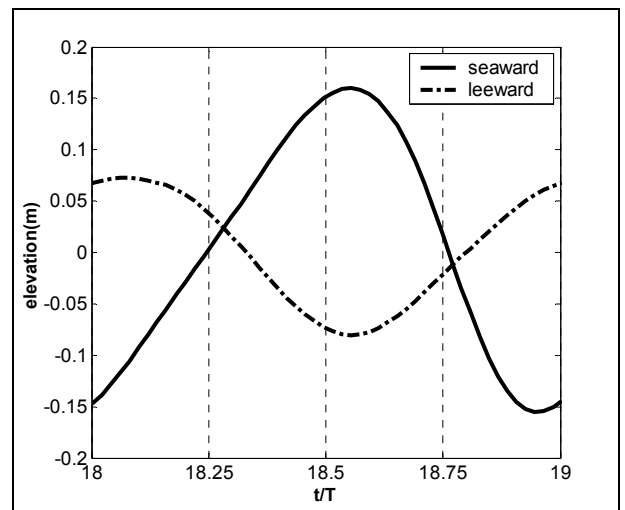


Fig. 8. Wave elevation at the two sides of the FB.

For  $Dr/D=0.2$  the  $C_t$  takes the highest value of 0.62 and the velocity vectors exhibit increased values in the vicinity of the FB and at the leeward vertical barrier, as compared with those for higher  $Dr/D$ .

For phase a, the flow pattern is more intense in the front vertical barrier with maximum values for the velocities of 1.15 m/sec decaying for a distance about  $1 Dr$  to small values of 0.10m/sec. In the area near the rear barrier the velocities are about half the size with maximum value of 0.65m/sec. The direction of velocity vectors is opposite in the two vertical barriers, with the water masses moving seaward from the front barrier and leeward from the rear one. In the next phase b, the velocity field is milder in the area of two barriers, but maximum velocities occur underneath the deck and in the seaward side of the structure. For phase c the maximum velocities occur in the area underneath the rear barrier with maximum values of 0.80m/sec. For this phase the water mass is entering underneath the structure from both sides. In the last phase d, the velocities are highly increasing near the front barrier with that near the rear barrier diminishing.

In general the flow pattern consists of the interaction of the partial standing wave seaward the structure and the water mass ‘trapped’ between the two barriers. The disturbance is transmitted underneath the deck through the above mentioned flow mechanism, without particular resistance from the FB, showing that FBs with such small values of  $Dr/D$  are insufficient to prevent the wave transmission.

The effect of increased  $Dr/D$  is clearly seen by examining Fig.10 and 11, where the velocity field for a FB with  $Dr/D=0.40$  is shown for phases c and d. The flow mechanism is the same but for this configuration the front barrier is much more efficient in blocking the disturbance, so the elevation underneath the deck is very small. Velocities in the vicinity of the rear barrier are very low resulting in a much smaller transmitted wave. High velocities occur only in the seaward face of the FB and below the front barrier but they are still smaller than those of the FB with  $Dr/D=0.20$ .

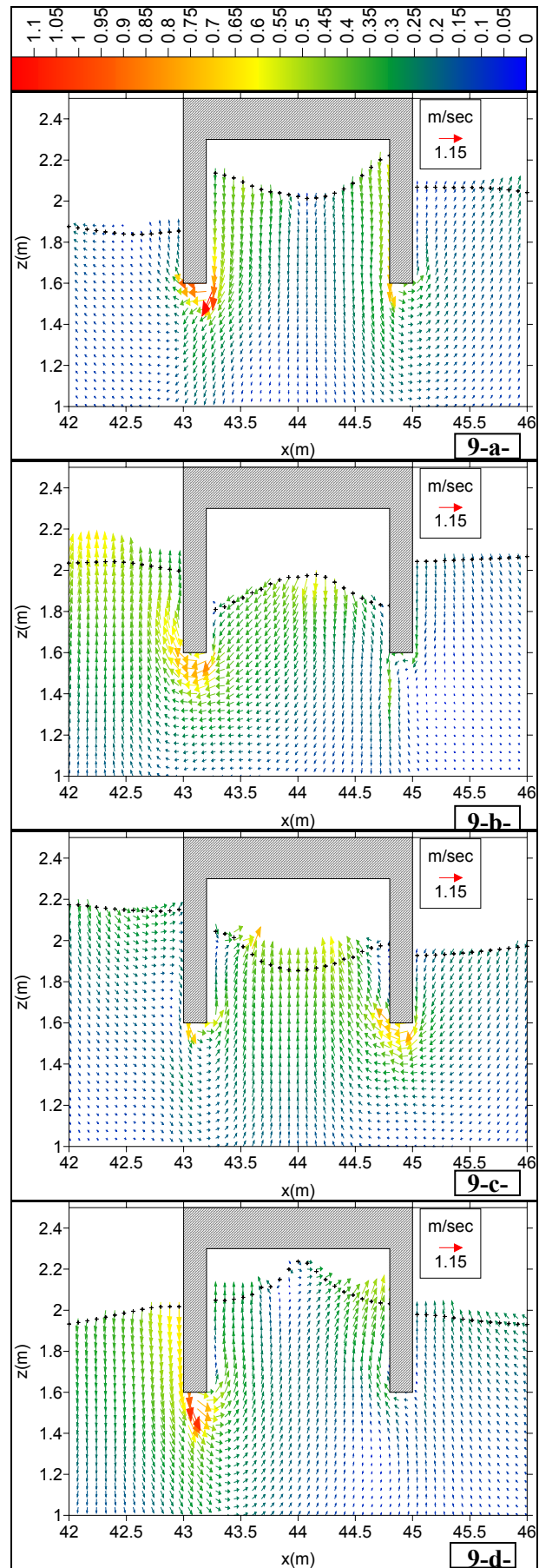


Fig. 9 (a-d). Velocity field for phases a-d

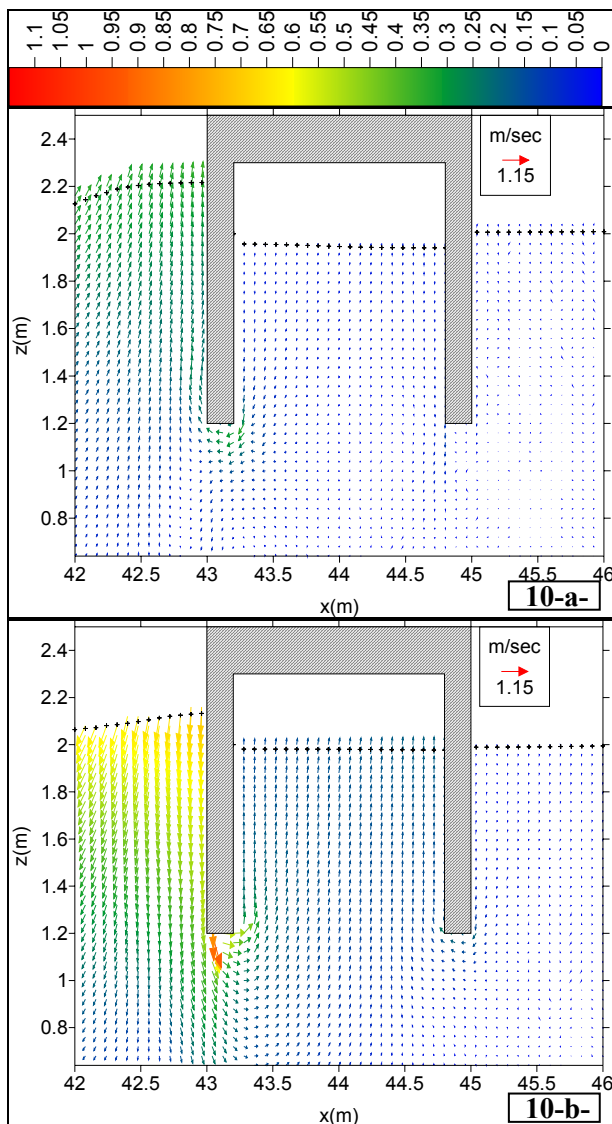


Fig. 10(a-b). Velocity field for phases c ( $t/T=0.50$ ) and d ( $t/T=0.75$ ) – $Dr/D=0.40$

#### 4 Conclusions

A numerical investigation on the effectiveness of a catamaran type FB under regular waves, with the use of a 2DV URANS model was carried out. The study was focused on the effect of the relative depth of immersion of the vertical barriers and the distance between them on wave reflection and transmission. It is found that the performance of the FB is highly improved with the increase of  $Dr/D$ , the relative depth of immersion. Low values for the transmission coefficient  $C_t$  (less than 0.1) are obtained for  $Dr/D > 0.4$ . Comparison between a catamaran and a box FB showed that the influence of  $Dr/D$  is stronger for a catamaran FB. The effect of  $S/L$ , relative spacing between the two barriers, on the  $C_t$ , is not significant and resonant phenomena are observed for  $S/L = n/2$ , ( $n=1,2,3\dots$ ).

#### Acknowledgement

The authors acknowledge the financial support of the Hellenic General Secretariat for Research and Technology (G.S.R.T.) through the program “Environmental Coastal Management with the use of Floating Breakwaters.

#### References:

- [1] Bruce, L., McCartney, M., Floating breakwater design, *Journal of Waterway, Port, Coastal and Ocean Engineering*, Vol.111, No.2, 1985, pp. 304-318.
- [2] Isaacson, M., Wave Effects on Floating Breakwaters, *Proceedings of Canadian Coastal Conference*, Vancouver, Canada, 1993, pp. 53-65.
- [3] Koutandos, E., Prinos, P., Gironella, X., Floating breakwaters under regular and irregular wave forcing: reflection and transmission characteristics, *Journal of Hydraulic Research*, Vol.43, No.2, 2005, pp. 174-188.
- [4] Isaacson, M., Baldwin, J., Premasiri, S., Yang, G., Wave interactions with double slotted barriers, *Applied Ocean Research*, Vol.21, No.2, 1999, pp.81-91.
- [5] Neelamani, S., Vedagiri, M., Wave interaction with partially immersed twin vertical barriers, *Ocean Engineering*, Vol.29, No.2, 2002, pp.215-238.
- [6] Liu, L.-F. P., Lin, P., *A numerical model for breaking waves: The Volume of Fluid Method*, Research Report. No. CACR-97-02, Center for Applied Coastal Research, Ocean Engineering Laboratory, University of Delaware. 1997.
- [7] Hirt, C.W., Nichols, B.D., Volume of Fluid (VOF) Method for the Dynamics of Free Boundaries, *Journal of Computational Physics*, Vol.39, No.1, 1981, pp.201-225.
- [8] Lin, P., Liu, L.-F. P., A numerical study of breaking waves in the surf zone, *Journal of Fluid Mechanics*, Vol.359, 1998, pp.239-264.
- [9] Lin, P., Liu, L.-F. P., Internal wave-maker for Navier-Stokes equation models, *Journal of Waterway, Port, Coastal and Ocean Engineering* Vol.125, No.4, pp.207-215.
- [10] Chorin, A.J. Numerical solution of the Navier-Stokes equations, *Mathematics of Computation*, Vol.22, 1968, pp.745-762.